Confocal Raman Microscopy Investigation of Phospholipid Monolayers Deposited on Nitrile-Modified Surfaces in Porous Silica Particles

David A. Bryce, Jay P. Kitt, Grant J. Myres, and Joel M. Harris*

Department of Chemistry, University of Utah, 315 South 1400 East,
Salt Lake City, UT 84112-0850 USA

ABSTRACT

Phospholipid bilayers deposited on a variety of surfaces provide models for investigation of lipid membrane structure and supports for biocompatible sensors. Hybrid supported-phospholipid bilayers (HSLBs) are stable membrane models for these investigations, typically prepared by self-assembly of a lipid monolayer over an n-alkane modified surface. HSLBs have been prepared on n-alkyl-chain modified silica and used for lipophilicity-based chromatographic separations. The structure of these hybrid bilayers differs from vesicle membranes, where the lipid head-group spacing is greater due to interdigitation of the lipid acyl chains with the underlying n-alkyl chains bound to the silica surface. This interdigitated structure exhibits a broader melting transition at higher temperature due to strong interactions between the lipid acyl chains and the immobile n-alkyl chains bound to silica. In the present work, we seek to reduce the interactions between a lipid monolayer and its supporting substrate by self-assembly of 1,2-dimyristoly-sn-glycero-3-phosphocholine (DMPC) on porous silica functionalized with nitrile-terminated surface ligands. The frequency of Raman scattering of the surface -C≡N stretching mode at the lipid-nitrile interface is consistent with an n-alkane-like environment and insensitive to lipid head-group charge, indicating that the lipid acyl chains are in contact with the surface-nitrile groups. The head-group area of this lipid monolayer was determined from the within-particle phospholipid concentration and silica specific surface area and found to be (54±2Å^2), equivalent to the head-group area of a DMPC vesicle bilayer. The structure of these nitrile-supported phospholipid monolayers was characterized below and above their melting transition by confocal-Raman microscopy and found to be nearly identical to DMPC vesicle bilayers. Their narrow gel-to-fluid-phase melting transition is equivalent to dispersed DMPC-vesicles, suggesting that the acyl-chain structure on the nitrile support mimics the outer leaflet structure of a vesicle membrane.

* Corresponding author: harrisj@chem.utah.edu

INTRODUCTION

Molecular interactions that occur at the interface between aqueous solution and phospholipid membranes play a key role in many biological processes. These processes range from passive uptake of small molecules to active processes such as endocytosis and cell-signaling. Given the range and importance of lipid membrane chemistry, considerable effort has been made to develop model phospholipid bilayers supported on a range of substrates.[1-6] A common approach to forming model membrane systems is the assembly of a phospholipid bilayer on a glass or silica substrate prepared either by fusion of phospholipid vesicles or Langmuir-Blodgett-Langmuir-Schaefer deposition of phospholipid on planar supports.[1,5-10] Planar-supported phospholipid bilayers have been employed in a variety of experiments for assessing bilayer structure,[11,12] investigating membrane interactions with peptides and proteins,[9,13-15] and providing membrane-like supports for ligand-binding experiments and biosensing.[4,10,16] To increase surface area for spectroscopic characterization of these structures, supported lipid bilayers have also been deposited by vesicle fusion onto the interior surfaces of porous alumina membranes[17-20] and porous silica particles.[21,22]

While supported lipid bilayers on glass and other oxide surfaces have seen numerous applications as membrane models, their structure is stable only if the distal leaflet remains in aqueous solution, and unless the lipids are polymerized, emergence from water into air will transfer the outer leaflet onto the air-water interface.[23] A more stable and easily-formed alternative to supported-lipid bilayers has been developed where an outer leaflet of lipid molecules is deposited as a monolayer on a proximal-leaflet of hydrophobic n-alkyl chains bound to a solid support. These hybrid-supported lipid bilayers are formed through the interaction of the acyl chains of the phospholipid monolayer with a hydrophobic support surface. They can be self-assembled on alkane-thiol monolayers on planar gold or silver substrates,[24-26] on n-alkyl-silane functionalized glass,[27] and on porous reversed-phase chromatographic silica surfaces.[28-36] These C_{18} alkyl-chain derivatized porous particles, dynamically modified with lipid-monolayers, have been shown to be useful for chromatographic separations based on lipophilicity. They exhibit solute retention for both small molecules and proteins that track the partitioning of these solutes into phospholipid vesicle bilayers.[28-33] The high surface areas of these particles have allowed Raman spectroscopy investigations of both the lipid-bilayer structure and its interactions with membrane-active molecules.[34-36]

The quality of supported lipid bilayers as models for membrane investigations depends on their organization, stability, and mobility, all of which can be influenced by their interactions with the supporting substrate. Hybrid-supported lipid bilayers on n-alkane-modified silica surfaces exhibit significant structural differences compared to lipid vesicle membranes, including

a 2.5-fold lower phospholipid density in the lipid leaflet when compared to a phospholipid vesicle membrane. This lower lipid density has been shown to arise from interdigitation of the acyl-chains of the deposited phospholipid layer and the underlying C_{18} chains of the functionalized silica support.[34] This interdigitated structure leads to a significantly broadened melting transition, indicating strong interactions between the lipid acyl chains and the immobile n-alkyl chains covalently-bound to the surface.[34]

Supported lipid bilayers on both planar and porous oxide supports also exhibit significant broadening of the main melting phase transition compared to vesicle membranes, which has been attributed to strong head-group interactions of the proximal leaflet with the underlying substrate.[37-41] One approach to mitigating these effects is to reduce substrate interactions by forming supported lipid bilayers over less-strongly interacting polymer cushions, which results in bilayers whose properties are nearly identical to vesicle membranes.[42-45] The success of reducing substrate effects in supported lipid bilayers with polymer cushions indicates that substrate-induced structural effects in hybrid-lipid bilayer structures on chromatographic silica surfaces might also be lowered by changing the chemistry of the support surface to deposit a phospholipid leaflet whose structure and properties more closely resemble a vesicle-membrane lipid bilayer. The strong interactions of phospholipids with C_{18} reversed-phase chromatographic silica surfaces likely arise from the hydrophobic, low-density, and long-chain n-alkyl ligands that lead to interdigitation.[34] Glass substrates functionalized with an nitrile-terminated alkyl-silane have previously been employed as surfaces to support glass-nanopore lipid membranes.[46] These nitrile-modified surfaces produce a nanopore-spanning lipid bilayer that exhibits no ion leakage, which differs from bare-glass supported nanopores that exhibit significant ion leakage arising from the trapped water layer between the surface-proximal lipid leaflets and glass surfaces.[46] The nitrile-modified glass-nanopore result is consistent with a monolayer of lipid with its acyl chains sealing against the nitrile-terminated surfaces of the glass-nanopore support.

In this work, we present the deposition and characterization of 1,2-dimyristoly-sn-glycero-3-phosphocholine (DMPC) deposited on the surfaces of nitrile-derivatized porous chromatographic silica. The covalently-bound nitrile layer in the support particles provides an internal standard for quantification of surface-associated lipid by confocal Raman microscopy. The interfacial structure, melting transition, and kinetics of formation of these nitrile-supported DMPC structures are characterized and compared to DMPC vesicle phospholipid bilayers in free solution and C_{18}-supported DMPC hybrid-bilayers. The goal of this work is to discover a support for stable lipid-monolayers, whose properties and structure more closely match those of a phospholipid vesicle membrane.

EXPERIMENTAL SECTION

Reagents and Materials Spherical, bare-silica YMC-SIL and nitrile-derivatized YMC-CN chromatographic silica particles used in this work were obtained from YMC America (YMC Corp., Allentown, PA). These particles were reported by the manufacturer to be derivatized with 3-nitrilepropyldimethylchlorosilane and end-capped with trimethylchlorosilane, with an average particle diameter of 5-μm and mean pore diameter of 30-nm. Their specific surface area was determined by nitrogen BET analysis (Porous Materials Inc., Ithaca, NY) to be 85.4 m^2/g. Water used in all experiments was filtered using a Barnstead GenPure UV water purification system (ThermoFisher Scientific, Waltham, MA) and had a minimum resistivity of 18.0MΩ·cm. 1,2-dimyristoly-sn-glycero-3-phosphocholine (DMPC), 1,2-dimyristoyl-sn-glycero-3-phospho-L-serine (DMPS), and 1-palmitoyl-2-oleoyl-sn-glycero-3-phosphocholine (POPC) were purchased from Avanti Polar Lipids, Inc. (Alabaster, AL), diluted into chloroform, and stored at -15°C until use. Chloroform (Chromasolv Plus, >99.9%), Sodium chloride (NaCl), Potassium Chloride (KCl) and Calcium Chloride ($CaCl_2$), 3-Nitrobenzenesulfonic acid (3-NBS), and 2-Amino-2-(hydroxymethyl)-1,3-propanediol (Tris), acetonitrile and hexadecane were purchased from Sigma-Aldrich (St. Louis, MO) and used without further purification.

Phospholipid deposition and characterization. The approach taken to deposit DMPC onto high-surface-area chromatographic supports has been described in detail previously.[21] In short, a DMPC film was deposited by evaporation from chloroform solution onto the surfaces of a glass vial and subsequently re-hydrated in Tris-buffered saline, with 5 mM $CaCl_2$ added to the buffer to destabilize the vesicles and promote membrane rupture[47] from a dispersion having a phospholipid concentration of 2 mg/mL. This dispersion was sonicated at a temperature above the DMPC vesicle phase transition (>30 °C) to form small, unilamellar vesicles. After sonication, the vesicles were mixed with YMC-CN particles to form a suspension of 1-mg particles per 2 mg DMPC and stirred above the DMPC melting transition for 12 hours. After mixing, the treated particles were separated from any remaining vesicles by several iterations of centrifugation and re-suspension in water.

To test for the presence of intact (unfused) vesicles within the pores of nitrile-derivatized particles, DMPC was deposited within particles as above, but with 50-mM 3-NBS tracer in the buffer solution from which the vesicles are prepared; this tracer remains entrapped within intact lipid vesicles below their membrane melting transition.[48] After the vesicle fusion step, the vesicle-particle suspension in the 3-NBS-containing buffer was cooled in an ice bath to below the vesicle bilayer melting transition and then diluted 1000-fold with 3-NBS-free buffer, such that Raman scattering from free-solution 3-NBS was not detectable. Surface coverages of DMPC

were determined by carbon analysis (MHW Laboratories, Phoenix, AZ). For carbon analysis, particles were prepared as above, and after washing away excess lipid with deionized water, the particle slurry was dried at ~120 °C overnight to remove water from the sample. A sample of the YMC-CN particles was also subjected to carbon and nitrogen analysis by MHW to determine the carbon fraction contributed by the support to the DMPC results above, as well as the nitrile-ligand surface coverage.

To assess the impact of substrate chemistry on the melting behavior of the phospholipid, DMPC deposited on the interior surfaces of 5-μm 30-nm pore diameter nitrile-functionalized particles was characterized by differential scanning calorimetry (DSC), along with dispersions of DMPC vesicles. Samples for DSC analysis were prepared with final phospholipid concentration of ~2.5 mg/mL, degassed under mild vacuum, and loaded into the calorimeter (VP-DSC, Microcal). The calorimeter cell temperature was lowered to 10°C and allowed to equilibrate for 15 min. Heat capacity versus temperature data were collected at a scan rate of 1°C/min.

Confocal Raman Microscopy. The Raman microscope has been described in detail elsewhere. Briefly, a 647.1-nm beam expanded Kr+ laser (Innova 90, Conherent Inc. Santa Clara, CA) was directed into a Nikon TE-300 inverted microscope frame (Nikon Instruments Inc., Melville, NY) and reflected off a dichroic beam splitter to overfill the rear aperture of a 1.4 NA, 100x oil-immersion objective (CFL PLAN APO, Nikon Inc., Melville, NY), focusing the laser beam to a diffraction limited spot in a sample. Scattered light from the sample was re-collected through the objective, transmitted through the dichroic beam splitter, collimated, and filtered by a high-pass filter, (Semrock, Rochester, NY). After filtering, the scattered light was focused through the entrance slit of a monochromator (500 IS, Bruker Corp., Billerica, MA), and dispersed onto a charge coupled device (CCD) detector (Andor iDus 420, Andor USA, South Windsor, CT) for spectral acquisition by a diffraction grating with 300 lines/mm blazed at 750 nm. The entrance slit of the monochromator was set to 50 μm to define the horizontal dimension of the confocal aperture, while the vertical dimension was defined by limiting acquisition to 3 pixel rows on the CCD chip (78 μm).[49]

Raman spectra were collected from the interior of individual chromatographic particles as follows: the laser focus was translated to the solution-coverslip interface, where reflected light from the laser spot is visible. This reflection of the focused spot was then translated to beneath the center of the particle of interest. The microscope objective was then raised vertically, bringing the particle perimeter into sharp focus and focusing the confocal probe volume at the particle center, where spectra were collected. Spectral data analysis was carried out using custom Matlab routines (Mathworks, Natick, MA). Generally, spectra were truncated to isolate spectral regions of interest, and baseline corrected by subtraction of a 5th order polynomial fit to baseline

(non-peak containing) regions of the spectrum. Well cells for confocal Raman microscopy were constructed by fixing a ~12-mm length of 10-mm i.d., 13-mm o.d. Pyrex glass tubing to a No. 1 glass coverslip with Devcon 5-min epoxy (ITW Devcon, Danvers, MA).

The deposited DMPC in the particle pore network was quantified using the surface-bound nitrile as an internal standard. Use of a surface-bound internal standard and free-solution standards to quantify surface-associated molecular populations has been described previously.[50] Briefly, a calibration standard of acetonitrile and DMPC in 50:50 isopropyl alcohol:water solution was used to determine the relative Raman scattering efficiencies of the phospholipid head-group C-N stretch and the C≡N stretch of nitrile groups on the surface. The resulting response factor, the surface coverage of nitrile groups (from elemental analysis), and the measured Raman scattering intensities of the phospholipid head-group C-N stretch and substrate C≡N nitrile stretch within the particle was used to quantify the accumulated DMPC on the surface. The reported lipid surface coverages and head-group areas represent average results from five randomly-selected particles, and the reported uncertainties are standard deviations of the average.

Temperature-controlled Raman microscopy experiments were carried out in a jacketed brass microscopy well cell, assembled with double-stick tape sandwiched between a No.1 coverslip and a custom machined brass top plate. A sample volume is created by cutting an opening in the double stick tape (3M, St. Paul, MN), which can be filled through a port in the brass top plate. This assembly is jacketed with a copper insulating block, where the temperature is controlled by recirculating flow from a heating/cooling water bath (Neslab RTE-111, Portsmouth, NH). To compare temperature-dependent spectra of nitrile-supported phospholipids with vesicle membranes, optical-trapping confocal-Raman experiments were carried out on DMPC vesicles prepared by extrusion. Lipid suspensions were prepared as above, except that final lipid concentration after re-hydration was reduced to 1 mg/mL by dilution, and vesicles were formed by 11-extrusions through track-etched polycarbonate membranes using an Avanti mini-extruder (Avanti Polar Lipids Inc., Alabaster, AL) maintained at 40°C. The vesicles were then transferred to the temperature-controlled microscopy cell, and spectra were collected from individual vesicles trapped in the focus of the excitation beam.[51,52] The spectra (normalized to the C-N head-group intensity) were compared to spectra from within-particle nitrile-supported lipids to examine structural differences at 12 and 30°C, well above and below the DMPC phase transition.

RESULTS AND DISCUSSION

Raman scattering from phospholipid deposited on nitrile-derivatized surfaces. Phospholipid deposition onto the surfaces of 30-nm pores of nitrile-functionalized silica surface is carried out by deposition from DMPC vesicles formed by sonication above the DMPC melting transition in 80:20 H_2O:D_2O solution. After equilibration of nitrile-functionalized porous silica particles with the phospholipid vesicle dispersion for 12-hours and removal of excess lipid, Raman spectra were collected from the center of individual nitrile-modified particles, where the scattering from D_2O serves a marker for the solution within the pores of the particle. The difference spectrum in Figure 1 shows displacement of D_2O (broad O-D stretch centered at ~2500 cm^{-1}) from the pores of the particle upon accumulation of phospholipid. The observed Raman scattering from phospholipid includes the choline head-group C-N stretch (715 cm^{-1}) and carbon-carbon and carbon-hydrogen modes from the lipid acyl chains, including the C-C stretching (~1050 – 1130 cm^{-1}), CH_2 twisting (1295 cm^{-1}), CH_2 bending (1440 cm^{-1}) and C-H stretching (~2840 – 2980 cm^{-1}) modes, respectively.[53-59] A small shift in the surface-nitrile -C≡N stretch is also apparent in the difference spectrum, indicating a change in the nitrile interfacial environment upon lipid deposition (see below).

The observation of phospholipid scattering from within the porous particles does not establish that the DMPC vesicles fuse and that lipid is deposited on the nitrile-modified surface. Given a typical ~20-nm diameter of sonicated vesicles,[60] the DMPC might be present as intact vesicles in the 30-nm diameter pores. To test for the presence of unfused vesicles, an equivalent experiment was conducted with vesicles containing 3-nitrobenzene-sulfonic acid (3-NBS) as a tracer. The charged sulfonate group of 3-NBS prevents its escape from vesicles with gel-phase phospholipid membranes.[48] Tracer-containing vesicles were formed by sonication of DMPC in a solution of 50-mM 3-NBS and allowed to interact with CN-silica particles for 12-hours, while maintaining the temperature above the DMPC vesicle phase transition (>30°C) as above. The suspension in 50-mM 3-NBS solution was cooled below the

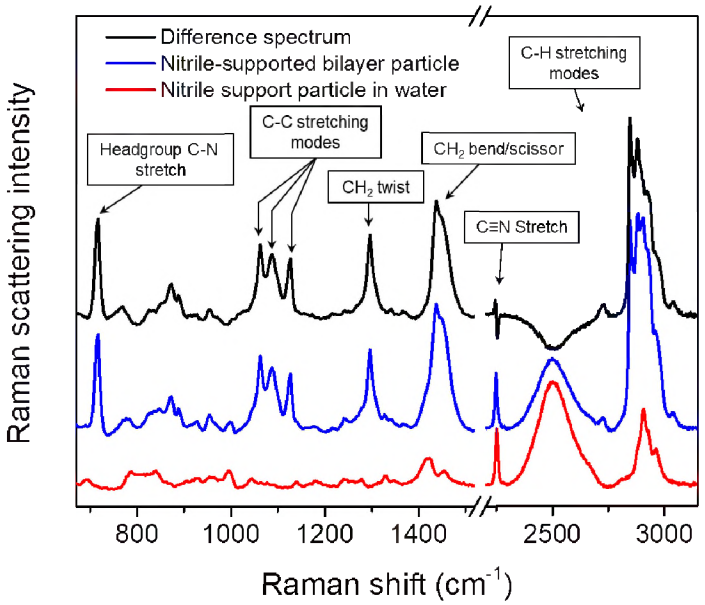

Figure 1. Raman spectra from a nitrile-support particle in water before (red) and after (blue) DMPC accumulation. Difference spectrum (black) shows phospholipid Raman bands, and a shift in the–C≡N stretching frequency (~2250 cm^{-1}) due to changes in the interfacial environment.

DMPC phase transition in an ice bath to seal the vesicle membranes from loss of tracer, and an aliquot of this suspension was diluted 1000-fold in an ionic-strength-matched buffer without 3-NBS; the diluted 3-NBS concentration is below the Raman scattering detection limit, so that any detectable 3-NBS must reside within intact vesicles. The dilute dispersion of particles was transferred to a cold cell, and Raman spectra were collected from both the lipid-containing particles and optically-trapped DMPC vesicles treated as above. Normalized spectra of optically-trapped vesicles and lipid-filled particles are compared in Figure 2, where the NO_2 symmetric-stretch of 3-NBS at 1359 cm^{-1} is clearly visible in optically-trapped vesicles, but totally absent in the spectrum from the lipid-containing particle. If the lipid within these particles derived from a significant population of intact DMPC vesicles, 3-NBS would be detected in the within-particle Raman spectra. The absence of the 3-NBS scattering indicates that the pore network is free of a significant population of intact vesicles so that the lipid signal derives from DMPC residing on the nitrile surface.

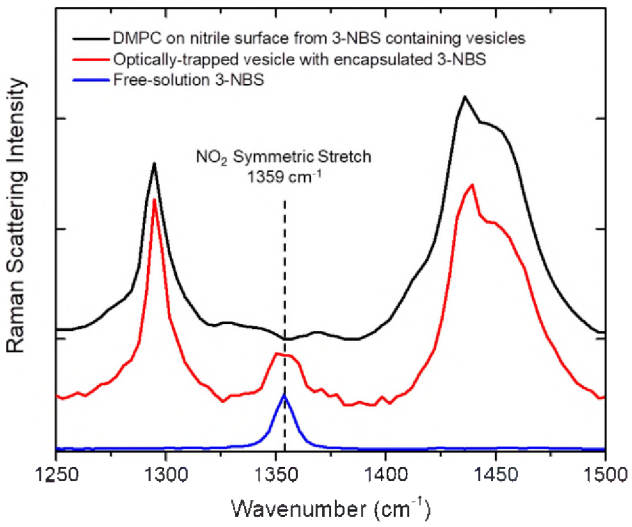

Figure 2. Evidence of vesicle-fusion during DMPC deposition. Spectra of a DMPC in a nitrile-silica particle following lipid-deposition with 3-NBS-filled vesicles (black), compared with an optically-trapped DMPC vesicle containing 50-mM 3-NBS (red); NO_2-symmetric-stretching mode is highlighted, flanked by CH_2 twisting and CH_2 bending/scissoring modes of the lipid acyl chains. Solution-phase 3-NBS spectrum for comparison (blue).

DMPC surface coverage. The DMPC layer on the interior surfaces of the CN-derivatized porous particles might exist as a supported phospholipid *bilayer* similar to lipid bilayers deposited by vesicle fusion onto planar glass[5,6,8,9] or bare porous alumina[17] or silica surfaces.[21] Another possibility is that a phospholipid *monolayer* is deposited, where lipid acyl chains contact the nitrile groups on the silica surface. This tails-down monolayer structure has been proposed for the lipid leaflets that adhere to the surfaces of nitrile-derivatized glass nanopores.[46] The lipids in contact with the nitrile surface showed no signs of a trapped water layer between the lipid and support surface as evidenced by no detectable ion leakage, which is observed with *bare-glass* nanopore supported bilayers.[46] The nitrile-modified glass-nanopore results are consistent with the acyl chains of the respective leaflets of the bilayer sealing against the nitrile-terminated surfaces of the nanopore support.

To assess whether the amount of deposited phospholipid corresponds to a lipid bilayer or monolayer, the deposited phospholipid was quantified by its Raman scattering intensity, using the surface nitrile-scattering as an internal standard based on its known surface coverage. A

Raman spectrum was acquired from a standard solution of acetonitrile (ACN) and DMPC in 50:50 isopropanol:water, and peak areas of the nitrile -C≡N stretch and phospholipid C-N head-group stretch were determined by fitting Voigt peak shapes to each of the peaks. The relative intensities of the phospholipid head-group C-N stretch (I_{C-N}^{soln}) and nitrile C≡N stretch ($I_{C\equiv N}^{soln}$) were used to calculate a conversion factor F using concentrations [*DMPC*] and [*Acetonitrile*] in the solution standard:

$$F = \frac{I_{C\equiv N}^{soln}}{I_{C-N}^{soln}} * \frac{[DMPC]}{[ACN]} \qquad (1)$$

This quantifies the relationship between the concentration of phospholipid and nitrile groups in a sample and the measured peak areas of the lipid C-N head-group and acetonitrile C≡N stretching modes. This conversion factor, F, can then be used to determine within-particle phospholipid surface coverage, Γ_{DMPC}:

$$\Gamma_{DMPC} = F * \Gamma_{C\equiv N} * \frac{I_{C-N}^{surf}}{I_{C\equiv N}^{surf}} \qquad (2)$$

based on the surface coverage of nitrile-groups within the particle, $\Gamma_{C\equiv N}$ = 3.4 μmol/m^2, determined from the mass fraction of nitrogen from elemental analysis, the nitrogen molecular weight of 3-nitrilepropyldimethylsilane, and the density of the support particles, from the specific pore volume and skeletal silica density. This nitrile surface coverage, $\Gamma_{C\equiv N}$, is used along with the measured intensities of the surface nitrile stretch, $I_{C\equiv N}^{surf}$, and phospholipid head-group C-N stretch, I_{C-N}^{surf}, to determine the surface coverage of DMPC in the particle interior, which is Γ_{DMPC} = 2.8±0.3μmol/m^2. This surface coverage can be compared to the surface coverage of nitrile silane, determined above, $\Gamma_{C\equiv N}$= 3.4 μmol/m^2, or approximately 1.2 nitrile groups per phospholipid.

The surface density of deposited DMPC was independently determined by carbon analysis. Carbon analysis was carried out on samples of nitrile-derivatized support particles (%$C_{support}$) as well as particles dried after deposition of phospholipid (%C_{sample}). The mass fraction of carbon added by the deposition of lipid (%C_{DMPC} = %C_{sample} - %$C_{support}$) can be used along with the carbon molecular weight of DMPC (MWC_{DMPC}) to calculate the mols of phospholipid deposited per gram of sample:

$$mol_{DMPC} = \frac{\%C_{DMPC} * 1g}{MWC_{DMPC}} \qquad (3)$$

The surface area of the sample can then be calculated using the specific surface area, *SSA*, of the support material, 85.4m^2/g, determined by nitrogen BET analysis, and the molecular weight of DMPC (MW_{DMPC}):

$$\Gamma_{DMPC} = \frac{mol_{DMPC}}{(1-\%C_{DMPC}*MW_{DMPC})*SSA} \qquad (4)$$

Here, the carbon analysis result, Γ_{DMPC} = 3.1 ±0.1 μmol/m^2, is in agreement with the coverage determined by Raman spectroscopy, above.

This phospholipid surface coverage in μmol/m^2 can be used to estimate the head-group area of a phospholipid in a monolayer by inverting its product with Avogadro's number, N_A:

$$Headgroup\ Area = (\Gamma_{DMPC} * N_A)^{-1} \qquad (5)$$

The calculated head-group area of a single DMPC lipid leaflet on the nitrile surface based on these results is 54±2 Å^2, which is in close agreement (~7% smaller and within the measurement uncertainties) with the value reported for a fluid-phase DMPC vesicle bilayer, measured by small-angle neutron scattering experiments on vesicle dispersions.[61] Thus, the calculated surface coverage of DMPC from these results is consistent with a lipid monolayer on the nitrile surface, in agreement with predictions based on minimal ion leakage with lipids on nitrile-derivatized glass nanopore supports.[46]

Surface-nitrile interfacial environment. While the amount of DMPC deposited within the particle is consistent with tails-down lipid monolayer, this proposed structure can be further tested by examining the environmentally-sensitive surface-nitrile -C≡N stretching frequency.[62] As shown in Figures 1 and 3, the nitrile stretching frequency exhibits a significant shift to lower frequency upon deposition of DMPC from water. The shift to lower frequency of the -C≡N stretching mode indicates that the accumulation of phospholipid produces a much lower dielectric constant interfacial environment.[62] This shift would therefore be consistent with formation of a tails-down phospholipid monolayer, where lipid acyl chains replace the water that was previously in contact with the nitrile groups on the silica surface. In Figure 3A, the Raman spectrum of the -C≡N stretching mode from surface nitriles with adsorbed DMPC is compared with the nitrile-derivatized particle immersed in water and n-heptane. DMPC produces a nearly-identical nitrile Raman spectrum as in n-heptane, in agreement with the tails-down monolayer structure proposed

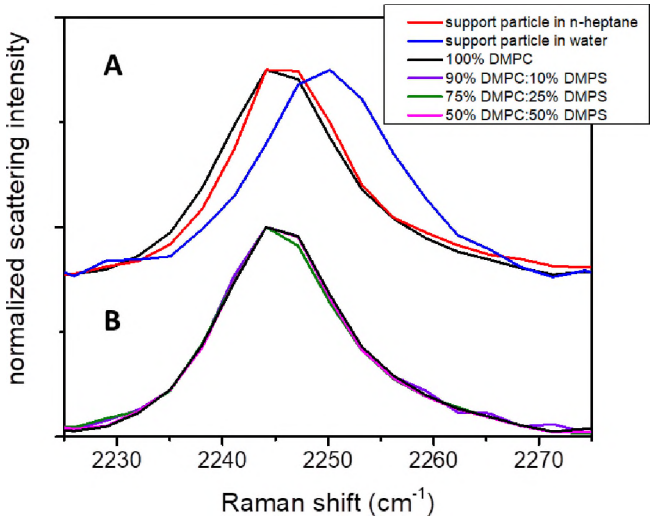

Figure 3. Raman spectra of the -C≡N stretching mode of the nitrile support particle. A. Scattering with deposited DMPC (black) compared with nitrile surface in contact with water (blue) and n-heptane (red). B. Nitrile stretching mode with DMPC (black), 90:10 DMPC:DMPS (violet), 75:25 DMPC:DMPS (green) and 50:50 DMPC:DMPS (pink). No head-group-charge-dependent shift in the -C≡N stretching frequency is observed.

for lipid monolayer leaflets on nitrile-derivatized glass nanopores.[46] The results in Figure 3A also support a conclusion that coverage of the underlying nitrile surface by the lipid monolayer is complete and not patchy. If there were significant regions of uncovered nitrile surface following lipid deposition, then Raman spectrum of the nitrile -C≡N mode would exhibit higher-frequency scattering characteristic of a bare, water-exposed nitrile surface (Figure 3A (blue)). The spectrum of the DMPC-covered surface (Figure 3A (black)) shows no detectable scattering in this higher frequency region, indicating that the nitrile surface is fully covered by lipid with minimal residual regions that remain exposed to the aqueous environment.

The conclusion reached above that DMPC adsorbs tails-down in a well-organized lipid monolayer can be further validated by testing the effects of lipid head-group charge on the substrate nitrile frequency. If a charged lipid is deposited as a bilayer or a poorly organized monolayer where the charged head-groups make contact with the surface nitriles, the -C≡N stretching frequency should show a Stark-shift[63-65] arising from a change in interfacial electric field arising from the proximity of the charged lipid head-groups. Lipid deposition on the nitrile-terminated surface was carried out using mixed phospholipid vesicles formed from 0, 10, 25, and 50 mol% negatively-charged 1,2-dimyristoyl-sn-glycero-3-phospho-L-serine (DMPS) in zwitterionic DMPC. Raman spectra of the substrate nitrile stretch for lipid compositions with a variable ratio of DMPC and DMPS particles are presented in Figure 3B. For all compositions of charged lipid (including 100% zwitterionic DMPC), the Raman spectra of the nitrile -C≡N stretch are equivalent, with a constant center frequency of 2245 cm^{-1} and no detectable Stark-tuning arising from the changes in the head-group charge. The lack of head-group charge sensitivity further supports the conclusion that the lipid is deposited as a well-organized tails-down monolayer with acyl chains in contact with the nitrile surface.

Organization and structure of nitrile-supported DMPC monolayers. Raman spectroscopy is a tool capable of providing information on the structure of phospholipid membranes.[12,66,67] Several phospholipid Raman-active vibrational modes are structurally informative and have been described in detail elsewhere.[34,57-59] Briefly, relative intensities of phospholipid acyl-chain carbon-carbon gauche- (1090 cm^{-1}) and trans-conformers (1061 cm^{-1} and 1127 cm^{-1}) are indicative of acyl-chain disorder in the phospholipid bilayer. Upon melting, a broadening of the CH_2 twisting mode (1296 cm^{-1}) is expected,[34,58] as well as disruption of long-range ordering in the acyl chains, which leads to a decrease in the intensity of the shoulder at ~1455 cm^{-1} observed in the CH_2 scissoring mode (1437 cm^{-1}).[59,68] The CH region of the spectrum comprises several overlapping Raman active modes, the relative intensity of which can be informative of acyl-chain order and packing density changes upon bilayer melting. To assess the structural similarities between nitrile-supported phospholipid monolayer with vesicle bilayers

in free solution, Raman spectra were collected from DMPC monolayers on the nitrile-modified particles as well as 400-nm diameter DMPC vesicles, both above and below the melting phase transition; these results are presented in Figure 4. Only one minor difference in the nitrile-supported lipid Raman spectrum is observed below the melting transition when comparing the supported monolayer to the vesicle bilayer: the shoulder observed in the CH_2 twisting modes is slightly more pronounced in the vesicle bilayer indicative of a greater disruption of long-range inter-chain coupling of the nitrile-supported lipid acyl-chains.[54,57,68]

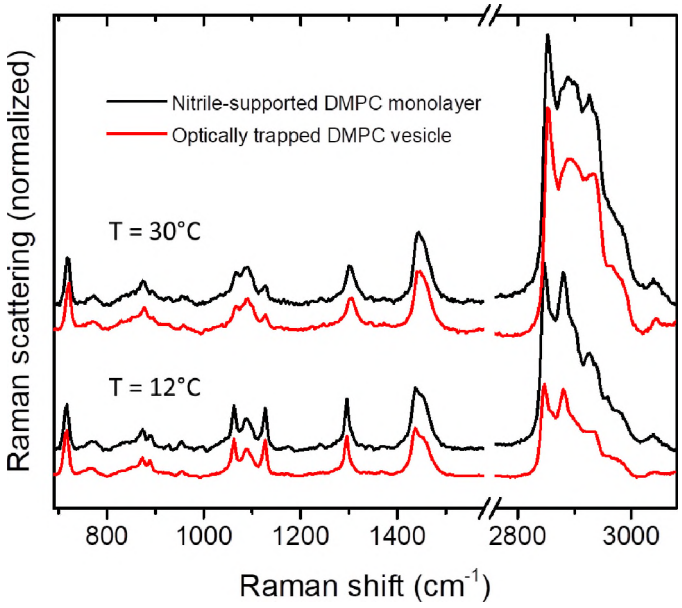

Figure 4. Raman spectra of nitrile-supported DMPC phospholipid monolayers in porous silica (black) and an optically-trapped DMPC vesicle bilayer (red) above and below the melting phase transition. Spectra are normalized to the phospholipid C-N head-group stretch at 715 cm^{-1}.

The carbon-hydrogen stretching region appears as a broad band comprising multiple Raman modes spanning the frequency range from ~2820 cm^{-1} to ~3020 cm^{-1}. Several bands in this region, the CH_2 symmetric stretching mode (2847 cm^{-1}) and antisymmetric stretching mode (2883 cm^{-1}), and the terminal CH_3-methyl stretching mode (2930 cm^{-1}) can be structurally informative, providing information about the acyl-chain inter-chain coupling, structural disorder and lateral packing density within the bilayer.[56,69,70] In particular, the relative intensity of the CH_2-antisymmetric-stretching-mode as compared to the CH_2-symmetric-stretching-mode (I_{2883}/I_{2847}) is indicative of dipolar coupling of adjacent phospholipid acyl chains in the bilayer.[54,71] Below the melting phase transition the I_{2883}/I_{2847} ratios for the nitrile-supported monolayer and vesicle bilayer are indistinguishable and are indicative of a well-ordered monolayer on the nitrile surface, consistent with the equivalent lipid packing density of this structure and a vesicle membrane. After exceeding the melting transition temperature, a small ~15% decrease in the I_{2883}/I_{2847} ratio for the nitrile-supported monolayer as compared to the vesicle bilayer is observed. This change suggests that inter-chain coupling is more significantly disrupted in the supported monolayer upon melting. This result, as well as the observed differences in the CH_2 scissoring mode (described above) may be the result of the topography of the pore network of the nitrile particle support to which the deposited phospholipid has conformed.[54,57,68 71,72]

Melting transition of nitrile-supported DMPC monolayers. Phospholipid bilayers of

dispersed vesicles typically exhibit a well-defined, sharp melting transition from an ordered gel phase to a disordered liquid crystalline phase.[73,74] At temperatures below the characteristic phase transition the lipid acyl chains adopt a predominantly trans-conformations, and develop a greater fraction of acyl-chain gauche conformations as the bilayer melts (see Figure 4).[34,58,59] The melting transition can also have dramatic effects on the dynamics of the phospholipid molecules[1,75] and also on the interactions and dynamics of molecules within the bilayer.[76] To investigate the impact of the substrate on the melting transition of nitrile-supported monolayers, differential scanning calorimetry (DSC) experiments were carried out, where the temperature-dependent heat capacity of a sample reports the progress through the melting transition of the sample.[77,78] Normalized DSC thermograms for a nitrile-supported DMPC monolayer and C_{18}-silica supported DMPC monolayer (hybrid bilayer)[34] are compared with DMPC lipid vesicles in Figure 5. DMPC on the C_{18}-silica surface exhibits a small peak previously observed in DSC endotherms of n-alkane supported hybrid bilayers,[79] which is likely a small fraction of multilayer lipid adsorbed to the hybrid bilayer, since the peak occurs at a temperature equivalent to the DMPC vesicle melting transition.[79] This is followed by a broad, high-temperature melting transition ranging from ~25 to 40°C as reported for DMPC hybrid bilayers on C_{18}-modified silica surfaces,[34,79] similar to the higher-temperature and broadened DMPC-hybrid-bilayer melting transition on planar octadecanethiol-modified gold surfaces.[80] The broad, high-temperature melting phase transition on C_{18}-modifed silica is attributed to chain interdigitation,[34] producing strong interactions between the hybrid bilayer upper leaflet of DMPC and the covalently-bound lower leaflet of C_{18} chains that inhibit chain melting and broaden the phase transition.

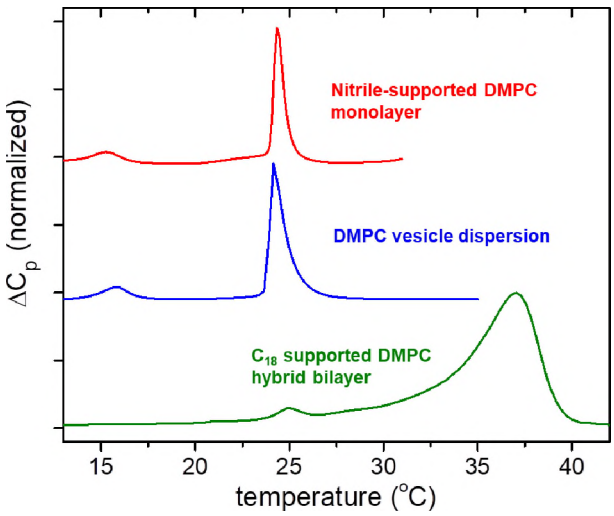

Figure 5. Differential scanning calorimetry (DSC) thermograms for a nitrile-supported DMPC monolayer (red), DMPC vesicles in suspension (blue), and a n-alkyl (C_{18}) supported DMPC hybrid bilayer (green).[34]

In contrast, the nitrile-supported DMPC monolayer melting appears as a single, narrow phase transition at 24.4°C, which is within the uncertainty of the measured main melting phase transition observed for dispersions of DMPC vesicles, 24.2°C (Figure 5), comparable to previous DSC results for DMPC vesicles in the literature, 23.5°C.[73] These results indicate a negligible impact of the nitrile-support substrate on the acyl-chain melting of the deposited lipid monolayer, with virtually identical pre-transition and main transition-temperatures and transition-widths

compared to vesicle membranes. The narrow melting transition of DMPC on the nitrile surface suggests weaker interactions of the lipid acyl chains with the underlying surface comparable to vesicle bilayers. The lipid monolayer on the nitrile surface appears to be a better model of vesicle bilayer leaflet compared to lipid monolayers on alkyl chain (C_{18}) silica surfaces (hybrid bilayers), where interdigitation and entanglement of the lipid acyl chains and covalently bound C_{18}-chains leads to a broad and higher-temperature melting transition.

The nitrile-supported DMPC monolayer exhibits a pre-transition at ~15.2°C that is equivalent to the pre-transition of vesicle lipid bilayers, ~15.7°C, and comparable to the literature DCS results for the pre-transition of DMPC vesicles,[81,82] 14.5°C. The observation of a similar pre-transition as a DMPC vesicle membrane is surprising, however, since x-ray diffraction[83] and freeze-fracture TEM[84,85] results and indicate that this transition is to a ripple-phase, where corrugations in the membrane are observed with periodicity on the scale of 10 to 30-nm. Molecular-dynamics simulations suggest these arise from fluid-phase defects in one leaflet of a bilayer that bend the membrane producing opposing regions of fluid- and gel-phase domains.[81] In a lipid monolayer, bending of the leaflet away from contact with the nitrile-surface would not be likely; however, the 30-nm diameter pores may support 30-nm-scale fluid- and gel-phase domains that occupy regions of the support surface having positive and negative curvature, respectively.

Conclusions. In this work, we have characterized DMPC deposited on surfaces of nitrile-derivatized porous silica particles, whose high specific surface area allows label-free confocal Raman spectroscopic investigation of their interfacial structure. The covalently-bound nitrile ligands are used as an internal standard for the quantification of the deposited phospholipid. The absence of unruptured vesicles and the interfacial environment of the surface nitrile groups indicate that the lipid assembles as a tails-down monolayer on the nitrile surface. The surface coverage of DMPC corresponds to a head-group area of the deposited phospholipid monolayer (54±2 Å^2) that is in good agreement with head-group spacing of DMPC vesicle membranes dispersed in solution. Additionally, the nitrile-supported lipid exhibits a narrow melting transition centered at 24.4°C equivalent to a DMPC vesicle bilayer melting transition. This behavior is significantly different than the broad and much higher-temperature melting transition of DMPC deposited on C_{18}-modified silica surfaces,[34,81] which arises from strong interactions and interdigitation of the lipid acyl chains with the covalently bound n-alkyl chains.[34] The nitrile-supported phospholipid monolayers exhibit similar phospholipid packing density, structure, and melting transition as the leaflets of a DMPC vesicle phospholipid bilayer, with minimal interactions between the lipid acyl chains and the nitrile-terminated support. These results suggest that phospholipid monolayers on nitrile-terminated supports may be promising for

lipophilicity-based small-molecule separations,[28-33] as a platform for lipid-supported ligands for biosensing or bioassays[4,10,16] or for spectroscopic investigations[36,86,87] of small-molecule interactions with a surface-supported but vesicle-like lipid monolayer.

ACKNOWLEDGMENTS

This material is based upon work supported by the U.S. Department of Energy, Office of Science, Office of Basic Energy Sciences, Division of Energy, Chemical Sciences, Geosciences, & Biosciences, Award Number DE-FG03-93ER14333; support for GJM from National Science Foundation, Grant CHE-1904424, is also acknowledged.

REFERENCES

(1) Tamm, L.K.; McConnell, H.M. Supported phospholipid bilayers. *Biophys. J.* **1985**, *47*, 105-113.

(2) Cremer, P.S.; Boxer, S.G. Formation and Spreading of Lipid Bilayers on Planar Glass Supports. *J. Phys. Chem. B* **1999**, *103*, 2554-2559.

(3) Wong, J.Y.; Majewski, J.; Seitz, M.; Park, C.K.; Israelachvili, J.N.; Smith, G.S. Polymer-cushioned bilayers. I. A structural study of various preparation methods using neutron reflectometry. *Biophys. J.* **1999**, *77*, 1445-1457.

(4) Yang, T.; Jung, S.-y.; Mao, H.; Cremer, P.S. Fabrication of Phospholipid Bilayer-Coated Microchannels for On-Chip Immunoassays. *Anal. Chem.* **2001**, *73*, 165-169.

(5) Richter, R.; Mukhopadhyay, A.; Brisson, A. Pathways of Lipid Vesicle Deposition on Solid Surfaces: A Combined QCM-D and AFM Study. *Biophys. J.* **2003**, *85*, 3035-3047.

(6) Richter, R.P.; Bérat, R.; Brisson, A.R. Formation of Solid-Supported Lipid Bilayers: An Integrated View. *Langmuir* **2006**, *22*, 3497-3505.

(7) McConnell, H.M.; Watts, T.H.; Weis, R.M.; Brian, A.A. Supported planar membranes in studies of cell-cell recognition in the immune system. *Biochim. Biophys. Acta, Rev. Biomembr.* **1986**, *864*, 95-106.

(8) Kalb, E.; Frey, S.; Tamm, L.K. Formation of supported planar bilayers by fusion of vesicles to supported phospholipid monolayers. *Biochim. Biophys. Acta, Biomembr.* **1992**, *1103*, 307-316.

(9) Leonenko, Z.V.; Carnini, A.; Cramb, D.T. Supported planar bilayer formation by vesicle fusion: the interaction of phospholipid vesicles with surfaces and the effect of gramicidin on bilayer properties using atomic force microscopy. *Biochim. Biophys. Acta, Biomembr.* **2000**, *1509*, 131-147.

(10) Castellana, E.T.; Cremer, P.S. Solid supported lipid bilayers: From biophysical studies to sensor design. *Surf. Sci. Rep.* **2006**, *61*, 429-444.

(11) Liu, J.; Conboy, J.C. Phase Transition of a Single Lipid Bilayer Measured by Sum-Frequency Vibrational Spectroscopy. *J. Am. Chem. Soc.* **2004**, *126*, 8894-8895.

(12) Lee, C.; Bain, C.D. Raman spectra of planar supported lipid bilayers. *Biochim. Biophys. Acta, Biomembr.* **2005**, *1711*, 59-71.

(13) Sezgin, E.; Schwille, P. Model membrane platforms to study protein-membrane interactions. *Mol. Membr. Biol.* **2012**, *29*, 144-154.

(14) Fox, C.B.; Wayment, J.R.; Myers, G.A.; Endicott, S.K.; Harris, J.M. Single-Molecule Fluorescence Imaging of Peptide Binding to Supported Lipid Bilayers. *Anal. Chem.* **2009**, *81*, 5130-5138.

(15) Myers, G.A.; Gacek, D.A.; Peterson, E.M.; Fox, C.B.; Harris, J.M. Microscopic Rates of Peptide–Phospholipid Bilayer Interactions from Single-Molecule Residence Times. *J. Am. Chem. Soc.* **2012**, *134*, 19652-19660.

(16) Jung, H.; Robison, A.D.; Cremer, P.S. Multivalent Ligand-Receptor Binding on Supported Lipid Bilayers. *J. Struct. Biol.* **2009**, *168*, 90-94.

(17) Gaede, H.C.; Luckett, K.M.; Polozov, I.V.; Gawrisch, K. Multinuclear NMR Studies of Single Lipid Bilayers Supported in Cylindrical Aluminum Oxide Nanopores. *Langmuir* **2004**, *20*, 7711-7719.

(18) Wattraint, O.; Warschawski, D.E.; Sarazin, C. Tethered or Adsorbed Supported Lipid Bilayers in Nanotubes Characterized by Deuterium Magic Angle Spinning NMR Spectroscopy. *Langmuir* **2005**, *21*, 3226-3228.

(19) Chekmenev, E.Y.; Gor'kov, P.L.; Cross, T.A.; Alaouie, A.M.; Smirnov, A.I. Flow-Through Lipid Nanotube Arrays for Structure-Function Studies of Membrane Proteins by Solid-State NMR Spectroscopy. *Biophys. J.* **2006**, *91*, 3076-3084.

(20) Mager, M.D.; Almquist, B.; Melosh, N.A. Formation and Characterization of Fluid Lipid Bilayers on Alumina. *Langmuir* **2008**, *24*, 12734-12737.

(21) Bryce, D.A.; Kitt, J.P.; Harris, J.M. Confocal-Raman Microscopy Characterization of Supported Phospholipid Bilayers Deposited on the Interior Surfaces of Chromatographic Silica. *J. Am. Chem. Soc.* **2018**, *140*, 4071-4078.

(22) Bryce, D.A.; Kitt, J.P.; Harris, J.M. Confocal Raman Microscopy for Label-Free Detection of Protein–Ligand Binding at Nanopore-Supported Phospholipid Bilayers. *Anal. Chem.* **2018**, *90*, 11509-11516.

(23) Ross, E.E.; Bondurant, B.; Spratt, T.; Conboy, J.C.; O'Brien, D.F.; Saavedra, S.S. Formation of Self-Assembled, Air-Stable Lipid Bilayer Membranes on Solid Supports. *Langmuir* **2001**, *17*, 2305-2307.

(24) Plant, A.L. Self-assembled phospholipid/alkanethiol biomimetic bilayers on gold. *Langmuir* **1993**, *9*, 2764-2767.

(25) Plant, A.L.; Brighamburke, M.; Petrella, E.C.; Oshannessy, D.J. Phospholipid/Alkanethiol Bilayers for Cell-Surface Receptor Studies by Surface Plasmon Resonance. *Anal. Biochem.* **1995**, *226*, 342-348.

(26) Plant, A.L. Supported Hybrid Bilayer Membranes as Rugged Cell Membrane Mimics. *Langmuir* **1999**, *15*, 5128-5135.

(27) Linseisen, F.M.; Hetzer, M.; Brumm, T.; Bayerl, T.M. Differences in the physical properties of lipid monolayers and bilayers on a spherical solid support. *Biophys. J.* **1997**, *72*, 1659-1667.

(28) Hanna, M.; de Biasi, V.; Bond, B.; Salter, C.; Hutt, A.J.; Camilleri, P. Estimation of the partitioning characteristics of drugs: a comparison of a large and diverse drug series utilizing chromatographic and electrophoretic methodology. *Anal. Chem.* **1998**, *70*, 2092-2099.

(29) Krause, E.; Dathe, M.; Wieprecht, T.; Bienert, M. Noncovalent immobilized artificial membrane chromatography, an improved method for describing peptide-lipid bilayer interactions. *J. Chromatogr. A* **1999**, *849*, 125-133.

(30) Hanna, M.; de Biasi, V.; Bond, B.; Camilleri, P.; Hutt, A.J. Biomembrane lipids as components of chromatographic phases: Comparative chromatography on coated and bonded phases. *Chromatographia* **2000**, *52*, 710-720.

(31) Tsirkin, I.; Grushka, E. Characterization of dynamically prepared phospholipid-modified reversed-phase columns. *J. Chromatogr. A* **2001**, *919*, 245-254.

(32) Ollila, F.; Halling, K.; Vuorela, P.; Vuorela, H.; Slotte, J.P. Characterization of Flavonoid–Biomembrane Interactions. *Arch. Biochem. Biophys.* **2002**, *399*, 103-108.

(33) Godard, T.; Grushka, E. The use of phospholipid modified column for the determination of lipophilic properties in high performance liquid chromatography. *J. Chromatogr. A* **2011**, *1218*, 1211-1218.

(34) Kitt, J.P.; Harris, J.M. Confocal Raman Microscopy of Hybrid-Supported Phospholipid Bilayers within Individual C18-Functionalized Chromatographic Particles. *Langmuir* **2016**, *32*, 9033-9044.

(35) Kitt, J.P.; Bryce, D.A.; Minteer, S.D.; Harris, J.M. Confocal Raman Microscopy Investigation of Self-Assembly of Hybrid Phospholipid Bilayers within Individual Porous Silica Chromatographic Particles. *Anal. Chem.* **2019**, *91*, 7790-7797.

(36) Kitt, J.P.; Bryce, D.A.; Minteer, S.D.; Harris, J.M. Confocal Raman Microscopy for in Situ Measurement of Phospholipid–Water Partitioning into Model Phospholipid Bilayers within Individual Chromatographic Particles. *Anal. Chem.* **2018**, *90*, 7048-7055.

(37) Keller, D.; Larsen, N.B.; Møller, I.M.; Mouritsen, O.G. Decoupled Phase Transitions and Grain-Boundary Melting in Supported Phospholipid Bilayers. *Phys. Rev. Lett.* **2005**, *94*, 025701.

(38) Feng, Z.V.; Spurlin, T.A.; Gewirth, A.A. Direct Visualization of Asymmetric Behavior in Supported Lipid Bilayers at the Gel-Fluid Phase Transition. *Biophys. J.* **2005**, *88*, 2154-2164.

(39) Charrier, A.; Thibaudau, F. Main Phase Transitions in Supported Lipid Single-Bilayer. *Biophys. J.* **2005**, *89*, 1094-1101.

(40) Seeger, H.M.; Marino, G.; Alessandrini, A.; Facci, P. Effect of Physical Parameters on the Main Phase Transition of Supported Lipid Bilayers. *Biophys. J.* **2009**, *97*, 1067-1076.

(41) Wu, H.-L.; Tong, Y.; Peng, Q.; Li, N.; Ye, S. Phase transition behaviors of the supported DPPC bilayer investigated by sum frequency generation (SFG) vibrational spectroscopy and atomic force microscopy (AFM). *Phys. Chem. Chem. Phys.* **2016**, *18*, 1411-1421.

(42) Sackmann, E. Supported Membranes: Scientific and Practical Applications. *Science* **1996**, *271*, 43.

(43) Sackmann, E.; Tanaka, M. Supported membranes on soft polymer cushions: fabrication, characterization and applications. *Trends Biotechnol.* **2000**, *18*, 58-64.

(44) Tanaka, M.; Sackmann, E. Polymer-supported membranes as models of the cell surface. *Nature* **2005**, *437*, 656-663.

(45) Mashaghi, S.; van Oijen, A.M. A versatile approach to the generation of fluid supported lipid bilayers and its applications. *Biotechnol. Bioeng.* **2014**, *111*, 2076-2081.

(46) White, R.J.; Ervin, E.N.; Yang, T.; Chen, X.; Daniel, S.; Cremer, P.S.; White, H.S. Single Ion-Channel Recordings Using Glass Nanopore Membranes. *J. Am. Chem. Soc.* **2007**, *129*, 11766-11775.

(47) Chanturiya, A.; Scaria, P.; Woodle, M.C. The Role of Membrane Lateral Tension in Calcium-Induced Membrane Fusion. *J. Membr. Biol.* **2000**, *176*, 67-75.

(48) Schaefer, J.J.; Ma, C.; Harris, J.M. Confocal Raman Microscopy Probing of Temperature-Controlled Release from Individual, Optically-Trapped Phospholipid Vesicles. *Anal. Chem.* **2012**, *84*, 9505-9512.

(49) Williams, K.P.J.; Pitt, G.D.; Batchelder, D.N.; Kip, B.J. Confocal Raman Microspectroscopy Using a Stigmatic Spectrograph and CCD Detector. *Appl. Spectrosc.* **1994**, *48*, 232-235.

(50) Kitt, J.P.; Harris, J.M. Confocal Raman Microscopy for in Situ Detection of Solid-Phase Extraction of Pyrene into Single C18–Silica Particles. *Anal. Chem.* **2014**, *86*, 1719-1725.

(51) Ashkin, A. Acceleration and Trapping of Particles by Radiation Pressure. *Phys. Rev. Lett.* **1970**, *24*, 156-159.

(52) Cherney, D.P.; Conboy, J.C.; Harris, J.M. Optical-Trapping Raman Microscopy Detection of Single Unilamellar Lipid Vesicles. *Anal. Chem.* **2003**, *75*, 6621-6628.

(53) Lippert, J.; Peticolas, W. Raman active vibrations in long-chain fatty acids and phospholipid sonicates. *Biochim. Biophys. Acta, Biomembr.* **1972**, *282*, 8-17.

(54) Wong, P.T.T. Raman Spectroscopy of Thermotropic and High-Pressure Phases of Aqueous Phospholipid Dispersions. *Annu. Rev. Biophys. Bioeng.* **1984**, *13*, 1-24.

(55) Wallach, D.F.; Verma, S.P.; Fookson, J. Application of laser Raman and infrared spectroscopy to the analysis of membrane structure. *Biochim. Biophys. Acta, Rev. Biomembr.* **1979**, *559*, 153-208.

(56) Levin, I.W.; Bush, S.F. Evidence for acyl chain trans/gauche isomerization during the thermal pretransition of dipalmitoyl phosphatidylcholine bilayer dispersions. *Biochim. Biophys. Acta, Biomembr.* **1981**, *640*, 760-766.

(57) Orendorff, C.J.; Ducey, M.W.; Pemberton, J.E. Quantitative Correlation of Raman Spectral Indicators in Determining Conformational Order in Alkyl Chains. *J. Phys. Chem. A* **2002**, *106*, 6991-6998.

(58) Fox, C.B.; Uibel, R.H.; Harris, J.M. Detecting Phase Transitions in Phosphatidylcholine Vesicles by Raman Microscopy and Self-Modeling Curve Resolution. *J. Phys. Chem. B* **2007**, *111*, 11428-11436.

(59) Schultz, Z.D.; Levin, I.W. Vibrational spectroscopy of biomembranes. *Annu. Rev. Anal. Chem.* **2011**, *4*, 343-366.

(60) Van Venetië, R.; Leunissen-Bijvelt, J.; Verkleij, A.J.; Ververgaert, P.H.J.T. Size determination of sonicated vesicles by freeze-fracture electron microscopy, using the spray-freezing method. *Journal of Microscopy* **1980**, *118*, 401-408.

(61) Kučerka, N.; Kiselev, M.A.; Balgavý, P. Determination of bilayer thickness and lipid surface area in unilamellar dimyristoylphosphatidylcholine vesicles from small-angle neutron scattering curves: a comparison of evaluation methods. *Eur. Biophys. J.* **2004**, *33*, 328-334.

(62) Rowlen, K.L.; Harris, J.M. Raman spectroscopic study of solvation structure in acetonitrile/water mixtures. *Anal. Chem.* **1991**, *63*, 964-969.

(63) Oklejas, V.; Sjostrom, C.; Harris, J.M. SERS Detection of the Vibrational Stark Effect from Nitrile-Terminated SAMs to Probe Electric Fields in the Diffuse Double-Layer. *J. Am. Chem. Soc.* **2002**, *124*, 2408-2409.

(64) Oklejas, V.; Sjostrom, C.; Harris, J.M. Surface-Enhanced Raman Scattering Based Vibrational Stark Effect as a Spatial Probe of Interfacial Electric Fields in the Diffuse Double Layer. *J. Phys. Chem. B* **2003**, *107*, 7788-7794.

(65) Staffa, J.K.; Lorenz, L.; Stolarski, M.; Murgida, D.H.; Zebger, I.; Utesch, T.; Kozuch, J.; Hildebrandt, P. Determination of the Local Electric Field at Au/SAM Interfaces Using the Vibrational Stark Effect. *J. Phys. Chem. C* **2017**, *121*, 22274-22285.

(66) Vincent, J.S.; Revak, S.D.; Cochrane, C.D.; Levin, I.W. Interactions of model human pulmonary surfactants with a mixed phospholipid bilayer assembly: Raman spectroscopic studies. *Biochemistry* **1993**, *32*, 8228-8238.

(67) Litman, B.J.; Lewis, E.N.; Levin, I.W. Packing characteristics of highly unsaturated bilayer lipids: Raman spectroscopic studies of multilamellar phosphatidylcholine dispersions. *Biochemistry* **1991**, *30*, 313-319.

(68) Schultz, Z.D.; Levin, I.W. Lipid Microdomain Formation: Characterization by Infrared Spectroscopy and Ultrasonic Velocimetry. *Biophys. J.* **2008**, *94*, 3104-3114.

(69) Wallach, D.F.H.; Verma, S.P.; Fookson, J. Application of laser Raman and infrared spectroscopy to the analysis of membrane structure. *Biochim. Biophys. Acta, Rev. Biomembr.* **1979**, *559*, 153-208.

(70) Hill, I.R.; Levin, I.W. Vibrational spectra and carbon–hydrogen stretching mode assignments for a series of n-alkyl carboxylic acids. *J. Chem. Phys.* **1979**, *70*, 842-851.

(71) Snyder, R.G.; Strauss, H.L.; Elliger, C.A. Carbon-hydrogen stretching modes and the structure of n-alkyl chains. 1. Long, disordered chains. *J. Phys. Chem.* **1982**, *86*, 5145-5150.

(72) Snyder, R.G.; Hsu, S.L.; Krimm, S. Vibrational spectra in the C ▪ H stretching region and the structure of the polymethylene chain. *Spectrochim. Acta, Part A* **1978**, *34*, 395-406.

(73) Marsh, D. *CRC Handbook of Lipid Bilayers*; CRC Press, 1990.

(74) Koynova, R.; Caffrey, M. Phases and phase transitions of the phosphatidylcholines. *Biochim. Biophys. Acta, Rev. Biomembr.* **1998**, *1376*, 91-145.

(75) John, K.; Schreiber, S.; Kubelt, J.; Herrmann, A.; Müller, P. Transbilayer movement of phospholipids at the main phase transition of lipid membranes: implications for rapid flip-flop in biological membranes. *Biophys. J.* **2002**, *83*, 3315-3323.

(76) Edidin, M. Rotational and translational diffusion in membranes. *Annu. Rev. Biophys. Bioeng.* **1974**, *3*, 179-201.

(77) Sturtevant, J.M. A scanning calorimetric study of small molecule-lipid bilayer mixtures. *Proc. Natl. Acad. Sci. U. S. A.* **1982**, *79*, 3963-3967.

(78) Kitt, J.P.; Bryce, D.A.; Harris, J.M. Calorimetry-Derived Composition Vectors to Resolve Component Raman Spectra in Phospholipid Phase Transitions. *Appl. Spectrosc.* **2016**, 0003702816652359.

(79) Käsbauer, M.; Bayerl, T.M. Synthetic Lecithin Monolayers on Hydrophobized Silica Supports Interdigitate with the Surface-Attached Alkyl Chains under Gel Phase Conditions. *Langmuir* **1999**, *15*, 2431-2434.

(80) Anderson, N.A.; Richter, L.J.; Stephenson, J.C.; Briggman, K.A. Determination of Lipid Phase Transition Temperatures in Hybrid Bilayer Membranes. *Langmuir* **2006**, *22*, 8333-8336.

(81) Heimburg, T. A Model for the Lipid Pretransition: Coupling of Ripple Formation with the Chain-Melting Transition. *Biophys. J.* **2000**, *78*, 1154-1165.

(82) Prenner, E.J.; Lewis, R.N.A.H.; Kondejewski, L.H.; Hodges, R.S.; McElhaney, R.N. Differential scanning calorimetric study of the effect of the antimicrobial peptide gramicidin S on the thermotropic phase behavior of phosphatidylcholine, phosphatidylethanolamine and phosphatidylglycerol lipid bilayer membranes. *Biochim. Biophys. Acta, Biomembr.* **1999**, *1417*, 211-223.

(83) Janiak, M.J.; Small, D.M.; Shipley, G.G. Nature of the thermal pretransition of synthetic phospholipids: dimyristoyl- and dipalmitoyllecithin. *Biochemistry* **1976**, *15*, 4575-4580.

(84) Meyer, H.W.; Dobner, B.; Semmler, K. Macroripple-structures induced by different branched-chain phosphatidylcholines in bilayers of dipalmitoylphosphatidylcholine. *Chem. Phys. Lipids* **1996**, *82*, 179-189.

(85) Schneider, M.F.; Marsh, D.; Jahn, W.; Kloesgen, B.; Heimburg, T. Network formation of lipid membranes: Triggering structural transitions by chain melting. *Proc. Natl. Acad. Sci. U. S. A.* **1999**, *96*, 14312-14317.

(86) Fox, C.B.; Horton, R.A.; Harris, J.M. Detection of Drug−Membrane Interactions in Individual Phospholipid Vesicles by Confocal Raman Microscopy. *Anal. Chem.* **2006**, *78*, 4918-4924.

(87) Fox, C.B.; Harris, J.M. Confocal Raman microscopy for simultaneous monitoring of partitioning and disordering of tricyclic antidepressants in phospholipid vesicle membranes. *J. Raman Spectrosc.* **2010**, *41*, 498-507.

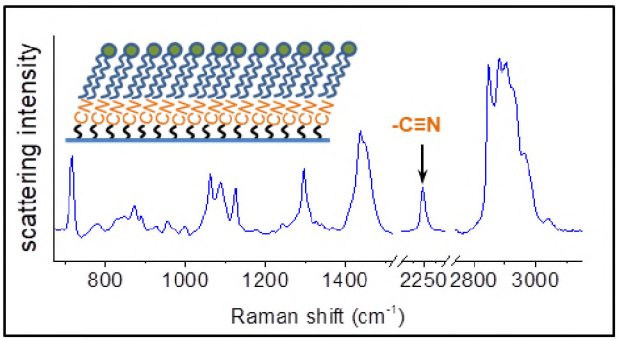
scattering intensity
-C≡N
800
1000
1200
1400
2250
2800
3000
Raman shift (cm-1)

TOC Graphic